The Membrane Skeleton of a Unicellular Organism Consists of Bridged, Articulating Strips

RONALD R. DUBREUIL and G. BENJAMIN BOUCK
Department of Biological Sciences, University of Illinois at Chicago, Chicago, Illinois 60680

ABSTRACT In this paper we show that a membrane skeleton associated with the plasma membrane of the unicellular organism *Euglena* consists of ~40 individual S-shaped strips that overlap along their lateral margins. The region of strip overlap is occupied by a set of microtubule-associated bridges and microtubule-independent bridges. Both cell form and plasma membrane organization are dependent on the integrity of this membrane skeleton. Removal of the membrane skeleton with a low-molar base results in loss of membrane form and randomization of the paracrystalline membrane interior characteristic of untreated cells. Conversely, removal of the plasma membrane and residual cytoplasm with lithium 3,5-diiodosalicylate/Nonidet P-40 yields cell ghosts that retain the form of the original cell but consist only of the membrane skeleton. Two major polypeptides of 86 and 80 kD persist in the skeleton and two other major proteins of 68 and 39 kD are associated with the plasma membrane fraction. None of these components appears to be the same as the major polypeptides (spectrins, band 3) of the erythrocyte ghost, the other cell system in which a well-defined peripheral membrane skeleton has been identified. We suggest that the articulating strips of euglenoids are not only the basic unit of cell and surface form, but that they are also positioned to mediate or accommodate surface movements by sliding, and to permit surface replication by intussusception.

Many euglenoids can undergo rapid changes in cell shape. Earlier suggestions (27) and recent evidence (57) indicate that these shape changes may be generated at the cell surface, thereby making this an especially interesting region of the motile cell. The surface of these euglenoids consists of alternating ridges and grooves that shift in orientation during cell deformation (2, 4, 22, 28, 37). The plasma membrane follows the contours of the ridges and grooves and is underlain by a closely adhering membrane skeleton. Previous studies have shown that when surfaces of *Euglena* are removed from other portions of the cytoplasm, they retain the native surface organization of ridges and grooves (22), although whole cell form is lost by fragmentation during isolation. At least three components of these surface isolates could in theory maintain surface and/or whole cell form: (*a*) The plasma membrane could dictate cell shape by a bilayer-couple mechanism (50) as resuggested for the erythrocyte (9, 12, 24, 25, 49). (*b*) The membrane skeleton could impose its own shape onto the plasma membrane, as proposed for the spectrin-rich membrane skeleton of the erythyrocyte (6, 23, 42, 51, reviewed in references 19 and 33). (*c*) The surface-associated microtubules may be responsible for whole cell shape, as previously suggested (13), although it seems unlikely that they are required for the maintenance of ridges and grooves (22).

In the present study we have first examined in detail the structural organization of the ridge and groove and have found that they consist of articulating S-shaped strips joined at their lateral edges by a complex bridgework of peglike attachments. The junction of these strips is the site of new strip insertion during intussusceptive surface growth. Second, we have selectively removed either the plasma membrane or the membrane skeleton and found that ridges and grooves as well as the paracrystallinity of the membrane interior are lost in isolated plasma membranes. Ridges and grooves, however, persist in the isolated membrane skeleton. The membrane skeleton also can by itself maintain the asymmetric shape of the whole cell. Third, since the membrane and the membrane skeleton can be separately analyzed, we have been able to characterize the major constituents of each fraction. It is clear that the proteins of the membrane skeleton have molecular weights and solubility properties unlike those of the cytoskeletal proteins reported for other systems. These results taken together suggest

THE JOURNAL OF CELL BIOLOGY · VOLUME 101 NOVEMBER 1985 1884-1896

that not only is the membrane skeleton of *Euglena* unique, but that it also provides a framework positioned to mediate the shape changes characteristic of this organism.

MATERIALS AND METHODS

Culture Maintenance: *Euglena gracilis* strain z was cultured and harvested as previously described (15).

Cell Surface Isolation and Purification: Log-phase cells were harvested from 500-ml cultures 3 d after inoculation, deflagellated by agitation in a fluted glass tube (48) or cold shock (47), and washed in culture medium and then centrifuged at low speed (1,000 *g*) for 5 min. Cell surfaces were purified on discontinuous sucrose gradients, using a procedure modified from reference 22. Deflagellated, washed cell pellets were resuspended in 3 ml buffer (10 mM *N*-2-hydroxyethyl-piperazine-*N*-2-ethanesulfonic acid, 25 mM KCl, pH 7.0; referred to throughout this article as HEPES buffer) with 1 g glass powder (5- or 25-μm diam, Heat Systems-Ultrasonics, Inc., Plainview, NY) to facilitate cell breakage. Two 10-s cavitations at the No. 4 setting of a Branson X125 Sonifier (Branson Instruments, Danbury, CT) separated by a short cooling interval resulted in complete cell disruption. Glass powder was then removed from the mixture by brief low-speed centrifugation. The sonicate was layered over 70% sucrose (wt/vol) in HEPES buffer and centrifuged in the SS-34 rotor of a Sorvall RC2-B centrifuge (DuPont Instruments, Sorvall Operations, Newtown, CT) at 17,500 rpm for 15 min. The resulting tightly packed pellet was resuspended in 1.5 ml HEPES buffer and then distributed to a discontinuous sucrose gradient of 85, 95, 100, and 110% sucrose (wt/vol) in HEPES buffer. After centrifugation for 90 min in a Beckman SW65 rotor (Beckman Instruments, Inc., Spinco Div., Palo Alto, CA) at 50,000 rpm a band of cell surface fragments was obtained at the 95–100% sucrose interface. The band was collected with a Pasteur pipette, resuspended in HEPES buffer, and recentrifuged at 40,000 rpm for 15 min. The resulting pellet consisted of nearly pure surface strips referred to here as surface isolates.

For electron microscopy cell surfaces were purified by density gradient centrifugation in Percoll (Sigma Chemical Co., St. Louis, MO) essentially as described by Murray (40). Deflagellated, washed cell bodies were resuspended in buffer (0.1 M piperazine-*N*,*N*′-bis(2-ethanesulfonic acid), 0.01 M EGTA, pH 7.0, referred to as PIPES buffer) and cavitated in the presence of glass powder as described above. Samples were layered over 50% Percoll (vol/vol) in PIPES buffer and centrifuged for 30 min in the SS-34 rotor at 17,500 rpm. A diffuse white band was removed from the gradient with a Pasteur pipette, resuspended, and washed several times in buffer, then subjected to a second Percoll fractionation. After several additional rinses in buffer, the purified cell surfaces were processed for electron microscopy.

Microscopy: Living cells were viewed with a Zeiss photomicroscope using Nomarski optics and a 1.25 numerical aperture planapochromat objective, and photographed with microflash illumination. For scanning electron microscopy cells from 50 ml culture solution were pelleted, frozen in liquid nitrogen, and then fixed in a solution containing 0.25% glutaraldehyde and 0.5% OsO_4 for 1 h at room temperature. Fixed cells were critical point dried in liquid freon and photographed in an ISI DS-130 scanning electron microscope (International Scientific Instruments Inc., Santa Clara, CA).

Surface isolates to be used for transmission electron microscopy were pelleted by centrifugation and fixed in 4% glutaraldehyde (Polysciences, Inc., Warrington, PA), 1% tannic acid (39) in 0.1 M PIPES buffer or 10 mM HEPES buffer. PIPES buffer gave significantly superior preservation and was used in all the preparations using thin sections in this report. After fixation for 1.5 h, the intact pellet was rinsed four times in buffer, postfixed in cold buffered 1% OsO_4 for 1 h, dehydrated in acetone, and flat embedded in Spurr's resin mixture (55). Sections of hardened blocks were stained in 1% uranyl acetate and then by lead citrate and then examined and photographed in a Hitachi 125A electron microscope.

For freeze-fracture studies, whole cells or isolated surfaces were fixed in 3% glutaraldehyde in 0.1 M sodium phosphate buffer, pH 7.4, for 1 h and infiltrated with 30% glycerol. A drop of cell suspension or of isolated surfaces was placed in a Balzers double replica apparatus and frozen in liquid nitrogen slush. Samples were fractured at −120°C in a Balzers BAF400T unit (Balzers, Hudson, NH) and shadowed with carbon-platinum. Replicas were cleaned in commercial bleach and mounted on Formvar-coated, carbon-stabilized copper grids.

Fractionation of Cell Surface Isolates and Preparation of Cell Ghosts: Extraction of isolates and all subsequent steps were carried out at 4°C except for lithium 3,5-diiodosalicylate (LIS)[1] treatments, which were performed at 25°C. Insoluble fractions were separated from the supernatant by centrifugation at 12,800 *g* for 10 min in an Eppendorf microcentrifuge (Brinkmann Instruments, Inc., Westbury, NY). Isolates were suspended in at least 100 vol of one of the following solutions: (*a*) LIS/Nonidet P-40 (NP-40): 25 mM LIS (Eastman Kodak Co., Rochester, NY), 1% NP-40 (Particle Data, Inc., Elmhurst, IL), and 5 mM EDTA in 10 mM Tris-HCl, pH 7.5; (*b*) NP-40: the same solution without LIS; (*c*) high salt: 0.6 M NaCl in 10 mM Tris-HCl, pH 7.5, 1 mM $CaCl_2$, 4 mM $MgCl_2$, 1 mM EDTA, and 7 mM β-mercaptoethanol; (*d*) base: 10 mM NaOH in distilled water; or (*e*) colchicine: 10^{-3} M colchicine in 0.1 M PIPES, pH 7.0.

Composition of Cell Surface Fractions: Surface isolates were divided into untreated, NaOH-soluble/insoluble and LIS/NP-40-soluble/insoluble fractions. Each fraction was sampled for total dry weight gravimetrically and for total protein (31) using bovine serum albumin (Sigma Chemical Co., St. Louis, MO) relyophilized before use as a standard. Averages were established from three experiments and all other tabulations were based on the average dry weight of the untreated fraction. Total lipids were weighed directly from chloroform/methanol extracts (22) in five separate experiments, and weight percentages were averaged and related to the untreated fraction dry weight. The percentage of neutral sugars was averaged from two experiments using dextran as a standard (10) and similarly related to the untreated fraction dry weight. All gravimetric analyses were made on a Cahn electrobalance (Cahn Instruments, Inc., Cerritos, CA) calibrated with a 10 mg standard with an accuracy of ±5 μg.

Gel Electrophoresis: Although the pattern of polypeptides revealed on modified Laemmli gels (26) was examined many times at various gel concentrations, all of the lanes shown in this report are from a single 9% slab gel and can be directly compared. Soluble samples were first precipitated in 90% acetone for 30 min at 0°C, then centrifuged at 15,000 *g*. Pellets were solubilized in sample buffer containing SDS by being heated for 2 min in a boiling water bath. The relative proportions of soluble and insoluble fractions were maintained in loading gels. After electrophoresis, polypeptide bands were stained in 0.25% Coomassie Brilliant Blue (in 50% ethanol/12% acetic acid) overnight, then destained in several changes of 10% ethanol/5% acetic acid. Quantitative scans of stained gel photographs were carried out with a Zeineh soft laser scanning densitometer (Biomed Instruments Inc., Chicago, IL). Molecular weight markers (Sigma Chemical Co.) included myosin heavy chain (205,000 mol wt), β-galactosidase (116,000 mol wt), phosphorylase a (97,400 mol wt), bovine serum albumin (66,000 mol wt), ovalbumin (45,000 mol wt), and carbonic anhydrase (29,000 mol wt).

RESULTS

Cells of *Euglena* undergo two kinds of external movements, which include "swimming" driven by the single emergent flagellum (during which cells maintain a more or less constant cigar shape) and "metaboly" or "euglenoid movement" during which cell shape changes dramatically. The cell deformations that accompany euglenoid movement are rapid (13, 28). This takes place as a wave of cell dilation progresses towards the anterior, and recovery results from cytoplasmic flow towards the cell posterior to initiate a new cycle (Fig. 1, *a–d*). Cell form during these movements may vary from nearly spherical to elongate and includes many intermediates.

Surface ridges and grooves are difficult to resolve using phase-contrast or Nomarski optics in this species but are evident in scanning electron microscope micrographs of selected stages of deformation (Fig. 1, *e–g*). As reported by earlier workers, the orientation of ridges, which is spiral in swimming cells, becomes nearly horizontal in spherical cells (Fig. 1 *e*), longitudinal in elongate cells, and adopts several different orientations in a single cell undergoing euglenoid movements (Fig. 1, *f* and *g*). The deformed cell retains its asymmetry after conversion to a ghost (Fig. 1, *h–j*) by incubation with LIS/NP-40 (see below). The ghost is a faithful shell of the original cell but shrinks substantially in overall volume under the extraction conditions used. Starch (paramylon) grains too large to escape through breaks introduced into the cell by freezing (to immobilize cells before extraction) are usually the only visible remains of cytoplasmic material in cell ghosts.

[1] *Abbreviations used in this paper:* LIS, lithium 3,5-diiodosalicylate; NP-40, Nonidet P-40.

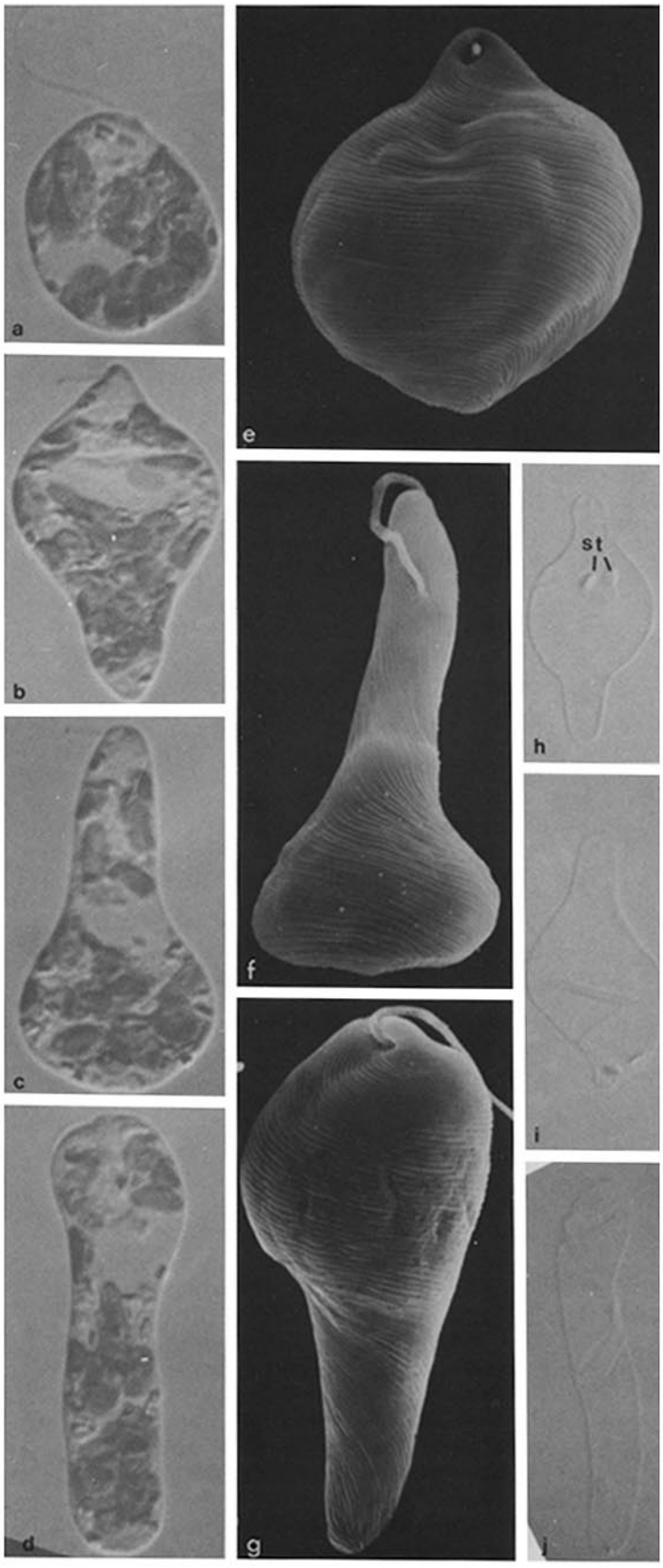

FIGURE 1 (*a–d*) Sequence of shape changes photographed at 5-s intervals of a cell undergoing euglenoid movements. The nearly spherical cell in *a* initiates a forward wave of dilation in *b*, which reaches the anterior of the cell (*b*, *top*), and then recovers by an inward flow of cytoplasm to initiate a new wave at *c*. The new wave progresses forward and the cell recovers in *d*. Scanning electron microscope micrographs in *e–g* illustrate the positions of the surface ridges and grooves during selected stages of deformation. Nearly horizontal strips in *e* reorient to longitudinal in cells initiating (*f*) or completing (*g*) a cycle. In *h–j* cell ghosts obtained by LIS/NP-40 extraction are seen to preserve the shape of the deformed cell, but a uniform decrease in size accompanies extraction. Occasional starch (paramylon) grains (*st*) are the only remnants of the original cytoplasm that remain in these ghosts. (*a–d*, *h–j*) × 2,060; (*e*) × 4,550; (*f*) × 3,720; (*g*) × 4,040.

Cell Surface Isolation

The ridge-and-groove organization of *Euglena* persists in cell-free surface isolates (22, Fig. 2*a*). Since the external face of the plasma membrane is free from a visible cell wall, surface organization must be molded either by the plasma membrane or its underlying cytoskeleton, or both. The results presented below suggest that it is the cytoskeleton alone that provides the structural framework of the euglenoid cell.

Isolation of cell surfaces by sucrose-density gradient centrifugation in HEPES or PIPES buffer yields a purified fraction virtually free of cytoplasmic material, but many important components of the surface complex cannot be clearly resolved. A similar deterioration of structural details occurs after isolation in metrizamide gradients (41). Percoll gradient centrifugation in PIPES buffer yields a surface fraction in which previously unrecognized details are evident. Percoll isolates, however, often contain remnants of cytoplasmic endoplasmic reticulum membranes, and Percoll itself seems to stick tenaciously to the inner surface of isolates even after repeated washes. Therefore, the cleaner sucrose gradient isolates have been used for all of the biochemical studies reported here, but Percoll gradients were used to resolve architectural details. A comparison of SDS gels of isolates from both preparative methods showed no significant differences in separated polypeptides (not shown).

Organization of the Overlapping Region

Representative thin sections of isolated cell surface are shown in Fig. 2, *a* and *b*, and details are shown diagrammatically in Fig. 3*b*. Although the plasma membrane is continuous along the ridge and groove, the membrane skeleton is discontinuous and in fact consists of individual parallel strips that overlap along their lateral margins. The junction between adjacent strips is particularly interesting and consists of well-defined complexes that link the right margin of one strip with the left margin of the adjacent more anterior strip. The occurrence of a junctional complex along the margin of each long strip provides a rationale for considering possible mechanisms of intussusceptive surface replication as well as a possible structural basis for surface movements (see Discussion). Hence, we have attempted to reconstruct the three-dimensional organization of the overlapping region and to identify by selective extraction a possible role for components at the junction.

Each parallel submembrane strip when viewed perpendicularly to its long axis is approximately S-shaped and encompasses one ridge and one groove (Fig. 3*c*). These strips spiral in about a 40-start helix of ~1.5 turns to form the undulating surface of the intact cell (Fig. 1, *e–g*, and 3*a*). Two bridges that join adjacent strips are attached to microtubules and are designated here as the microtubule-associated bridges of microtubules 1 and 2. Two other sets of bridges are not joined to microtubules and are designated as microtubule-independent bridges A and B. All of these bridges are cylindrical or oval in transverse section. They appear to be specialized extensions of the anterior edge of each strip which impinge on the inner surface of the neighboring strip (Fig. 2, *a* and *b*). Microtubule independent bridges-A, the most prominent of the bridges, are positioned along the strips with an average periodicity of ~137Å (three isolates). Microtubule independent bridges-B have a similar spacing of 143Å (three isolates), and microtubule-associated bridges-1 have an average periodicity of 150Å (one isolate). A third microtubule located at the strip margin is tightly appressed against a portion of the membrane skeleton and displays no obvious bridges. In addition to the precise bridging at the strip overlap, a series of traversing fibers (22) extends from the edge of one strip to the bottom of the neighboring strip groove (Fig. 2*b* and 3*b*). These fibers are attached perpendicularly to the long axis of each strip, with a mean periodicity that varied from 180 to 247Å (overall mean of 207Å) in the same preparations in which the bridges showed very uniform spacings. The traversing fiber appears to be positioned to act as an elastic spring between strips, which may account for the variation in spacing. In intact cells and occasionally in isolates a cisternum of the endoplasmic reticulum is found closely applied to this fiber (Fig. 2*b*).

Electrophoresis of solubilized surface isolates in SDS gels (Fig. 2*e*) separated a number of polypeptides, including two major components of 86 and 80 kD (Fig. 2*e*, lane *1*). These two polypeptides constitute ~30% of the proteins of surface isolates as determined by densitometric scans of gel photographs. The 86- and 80-kD bands are significantly enriched in surface isolates relative to the polypeptides of whole deflagellated cells (Fig. 2*e*, lane *2*). The 86-kD component is diminished and a higher molecular weight band appears when β-mercaptoethanol is omitted from the solubilization buffer (data not shown), which suggests a possible self-association of this polypeptide.

Effects of Salt and Colchicine on Microtubules

Since high ionic strength solutions (0.6 M NaCl) have been used to extract flagellar dynein arms and their ATPase activities (reviewed in reference 1), an attempt was made to remove the bridge structures from isolated surfaces by treatment with a high concentration of NaCl. After this treatment, central pair microtubules and dynein arms are completely removed from isolated *E. gracilis* flagellar axonemes (unpublished observation), but only microtubules 2 and 3 were consistently (and microtubule 1 variably) removed from cell surface isolates (Fig. 2*c*). Microtubule-independent bridges-A and -B remained intact and adjacent membrane skeletal strips were not dissociated. Electrophoresis of the NaCl extract (Fig. 2*e*, lane *3*) on SDS gels revealed two polypeptide bands that comigrate with flagellar tubulins between 50 and 55 kD, but no major high molecular weight dyneinlike proteins were apparent. The major 86- and 80-kD polypeptides remained associated with the insoluble pellet (Fig. 2*e*, lane *4*), comprising ~40% of total protein.

Colchicine at 10^{-3} M had no apparent effect on the microtubule complement in surface isolates (Fig. 2*d*). This is consistent with reports of the insensitivity of euglenoid cellular microtubules to this alkaloid (53), which indicates that they are of the "plant" type (21). Microtubule stability during isolation at 4°C supports this interpretation.

Effects of NaOH on Isolates

Because peripheral membrane proteins are generally soluble in base (56), attempts were made to remove the membrane skeleton by extraction with dilute NaOH. As expected, the submembrane layer was removed with 10 or 100 mM NaOH, leaving sheets of stripped plasma membranes (Fig. 4*d*). The ridge-and-groove surface organization was lost concomitantly

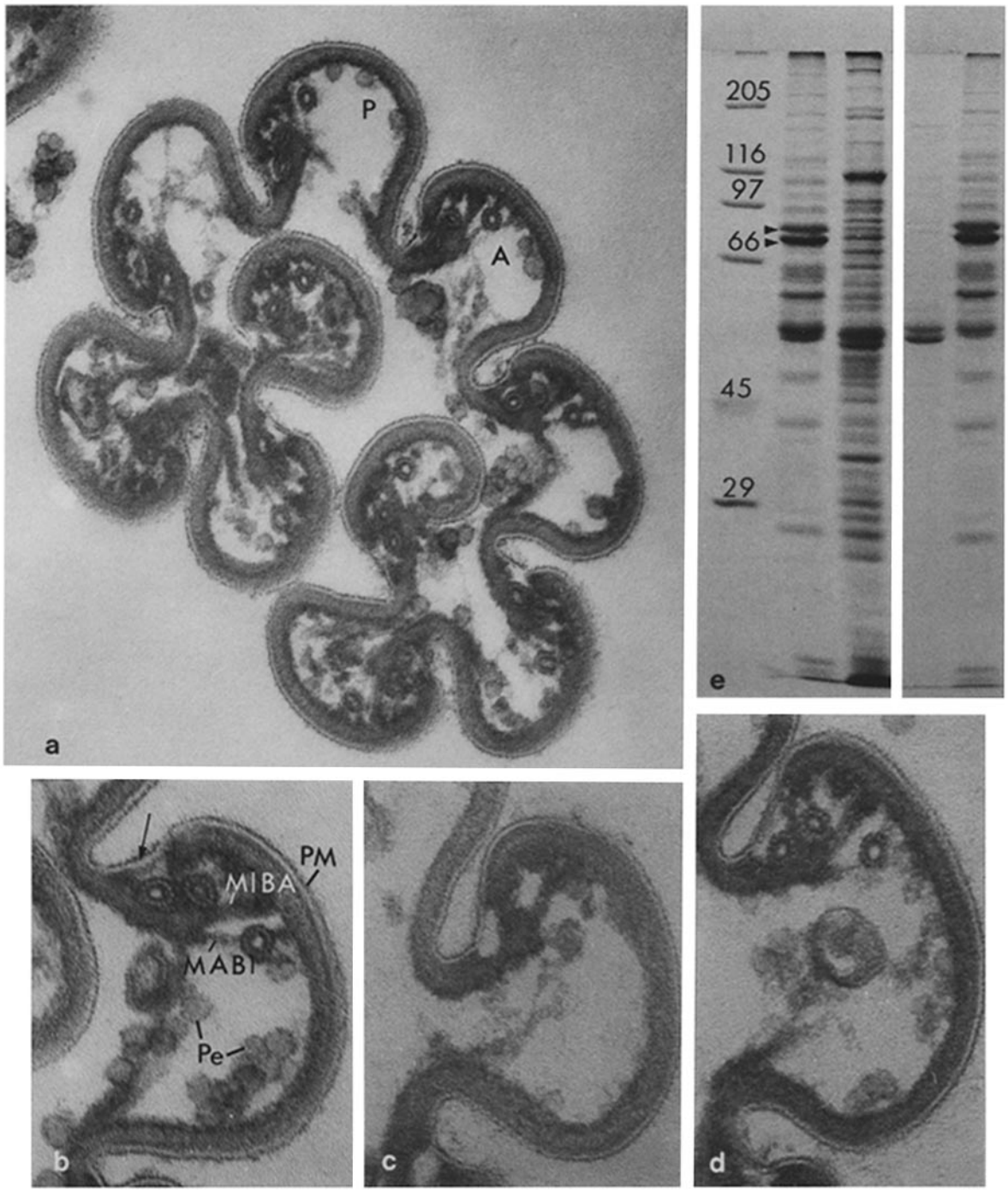

FIGURE 2 (*a* and *b*) Micrographs of cell surfaces isolated in Percoll gradients illustrating the membrane skeleton and bridgework. The plasma membrane (*PM*) is continuous over the ridge and groove, but the skeleton consists of laterally discontinuous strips appressed to the plasma membrane in all areas except at the strip junction in the groove (arrow). Although Percoll (*Pe*) sticks tenaciously to the inner surface of these preparations, the several sets of bridges can be readily identified. Microtubule-associated bridge-1 (*MAB1*) links the extreme lateral edge of the *P* (more posterior) strip to a point along the side of the *A* (more anterior) strip. The most prominent bridge is microtubule-independent bridge-A (*MIBA*), which forms a relatively thick connection from the edge of the *P* strip to a position along the side of the *A* strip. Other connections are described in the text. The polypeptides found in these isolates are shown in *e*, lane *1* (36 μg protein) and compared with total cellular polypeptides in *e*, lane *2* (10^5 whole deflagellated cells). Positions of molecular weight standards are shown to the left in thousands. Isolates are greatly enriched in two polypeptides of 86 and 80 kD (arrowheads), as well as in tubulin. Isolates extracted with 0.6 M NaCl lose most of their tubulin (lane *3*, 5 μg protein) and microtubules (*c*), but the MIBs remain intact, as does the ridge and groove organization. Lane *4* shows the composition of the salt-extracted surfaces (30 μg protein). The sample in lane *3* contains twice the amount of protein extracted from the material in lane *4*. (*d*) Colchicine (10^{-3} M) treatment of isolates has little obvious effect on microtubules or other structures. (*a*) × 130,000; (*b–d*) × 196,000.

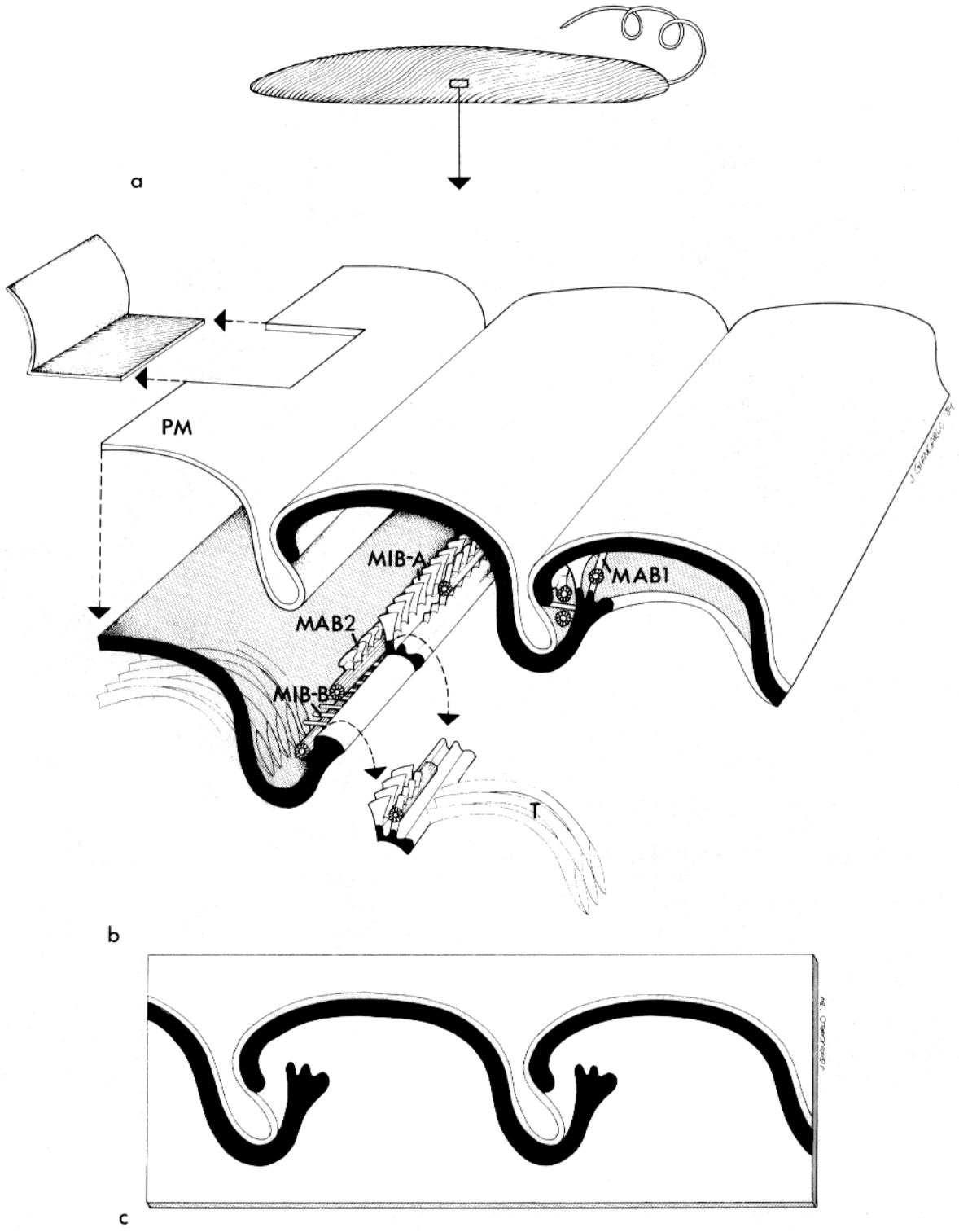

FIGURE 3 (a–c) Diagrams of a whole swimming cell (a) and transverse sections of the cell surface (*b* and *c*) illustrating details of the articulating S-shaped strips of the membrane skeleton and the infrastructure associated with strip overlap. The position of the skeleton and bridges seems well suited to mediate the sliding of adjacent strips that is presumed to occur during shape changes. The portion of the plasma membrane not subtended by the cytoskeleton may provide the fluid region, which accommodates sliding as well as a region for the insertion of new strips during surface replication. The traversing fiber is positioned to maintain the S-shaped configuration and it may contribute an elastic component to the sliding skeleton. *MAB1* and *MAB2*, microtubule-associated bridges; *MIB-A* and *MIB-B*, microtubule independent bridges; *PM*, plasma membrane; *T*, traversing fiber.

with the solubilization of the membrane skeleton. Solubilization of the stripped membranes followed by electrophoresis separated two major integral membrane proteins of 68 and 39 kD (Fig. 4*e*, lane *2*). That all of the other major proteins of surface isolates were present in the NaOH-soluble fraction (Fig. 4*e*, lane *2*) indicates that they are singly or collectively involved in maintaining ridge-and-groove organization. The 86- and 80-kD polypeptides account for ~35% of the NaOH-

extracted proteins (as determined by a densitometric scan of Fig. 4*e*, lane *1*).

Plasma membranes were examined by freeze fracturing before and after treatment with base. In whole cells, as described previously (29, 38), prominent striations consisting of intramembrane particles are evident in replicas of the external (EF) face of fractured plasma membranes (Fig. 4*b*). This organization persisted in isolated surfaces (Fig. 4*a*) but was not present after treatment with base (Fig. 4*c*). The striated EF fracture surface can be identified in these stripped membranes since the opposing protoplasmic face (PF) retains large granules that are artifacts of the relatively high temperature (−120°C) used for fracturing these membranes (38). In negatively stained preparations (not shown) as well as in fractured (Fig. 4*c*) and in sectioned (Fig. 4*d*) membranes, sealed vesicles were rare or nonexistent.

LIS/NP-40 Extraction Yields the Membrane Skeleton

The protein perturbant LIS is selective in the extraction of erythrocyte ghost membrane skeletons at low concentrations (<25 mM, reference 56) and disruptive to the plasma membrane at higher concentrations (0.3 M, reference 36). Therefore it seemed likely that the *Euglena* membrane skeleton would be removed from the plasma membrane by treatment with 25 mM LIS. Surprisingly, LIS by itself had relatively little effect, and NP-40 by itself produced only a microvesiculation of the plasma membrane. LIS and NP-40 together after overnight extraction, however, completely removed the plasma membrane and microtubules, leaving an insoluble membrane skeleton. Whole cell ghosts can also be obtained by this method (Fig. 1, *h–j*), although it is necessary to puncture cells by freezing to release insoluble cell contents such as starch grains. The apparent cytoskeletal ribs seen in the more detailed view (Fig. 5*b*) represent the laterally overlapping edges of individual strips. Sections of LIS/NP-40-treated isolates support this interpretation (Fig. 5, *a* and *c*). Despite the absence of the plasma membrane, microtubules, and microtubule-associated bridges, the membrane skeleton retains its intact articulating form.

The individual submembrane strips are linked to one another after LIS/NP-40 treatment primarily by the remaining microtubule-independent bridges, although the traversing fibers (Fig. 5*a*) may contribute to strip morphology. In some sections extension or stretching of adjacent strips is observed (Fig. 5*a*), which indicates some degree of flexibility in the basic framework. Yet for the most part, the original ridge and groove conformation of whole cells remains remarkably intact in these LIS/NP-40-treated isolates (Fig. 5, *a*, *c*, and *d*).

When the LIS/NP-40 membrane skeleton was solubilized in SDS and electrophoresed (Fig. 5*e*, lane *1*) it revealed a set of polypeptides that were nearly identical to those extracted by base (Fig. 4*e*, lane *2*). The 68- and 39-kD integral membrane proteins and a number of minor components were released after the plasma membrane was removed with LIS/NP-40 (Fig. 5*e*, lane *2*). The sample shown on the gel was extracted at 37°C for 1 h, but complete removal of the 68- and 39-kD polypeptides required at least 16 h of treatment. Two polypeptides that co-migrate with flagellar tubulins and a 25-kD polypeptide are present in the soluble extract and seem to be completely extracted after 1 h at 37°C. This solubilization corresponds with the loss of visible microtubules from surface isolates. The 86- and 80-kD polypeptides are the primary constituents of the membrane skeleton (~60% of total protein in a densitometric scan of Fig. 5*e*, lane *1*). The additional polypeptides may represent either the various bridges and fibers, accessory proteins, and/or cytoplasmic contaminants.

Composition of Cell Surface Isolates

The composition of each surface fraction is shown in Table I. The intact cell surface has a high protein/lipid ratio (5.1:1). After NaOH extraction, the membrane residue is substantially enriched in lipids and retains most of the carbohydrate of intact surface isolates. Conversely, the NaOH extract includes 85% of total isolate protein with little detectable lipid or carbohydrate. The dry weight of the LIS/NP-40-resistant fraction is difficult to determine accurately since it is the sum of the membrane skeleton weight plus an unknown amount of bound detergent (see below). The protein content of the LIS/NP-40-insoluble skeletons is lower than the protein content of NaOH-extracted peripheral proteins due to the enrichment of a subset of peripheral proteins in the former. Specifically, tubulin and a major 25-kD polypeptide are extracted with base but partition with the membrane fraction after LIS/NP-40 extraction.

The recovery of protein and carbohydrate from fractionated surfaces was essentially complete. The percentage of carbohydrate shown in Table I is about one-half of the previously reported value (22). This decrease is consistent with the results of a recent study (8) that shows that cultures of *Euglena* harvested at 4 d (22) have about twice as much carbohydrate as those harvested after 3 d (present study). The lipid content of untreated surfaces is in agreement with previous findings (22) although after NaOH extraction recovery was apparently not complete. If it is assumed that the unrecovered lipid is a part of the membrane fraction, the actual protein/lipid ratio of NaOH-extracted membranes would be ~0.8:1. The LIS/NP-40-soluble fraction was analyzed for neutral sugar and found to contain 4.5% of the untreated fraction dry weight

FIGURE 4 (*a–d*) Plasma membrane organization in intact cells (*b*), isolated surfaces (*a*), and NaOH-stripped membranes (*c* and *d*). Freeze-fracture replicas of whole cell surfaces display the prominent intramembrane EF surface striations characteristic of the plasma membrane over the surface ridges (see Fig. 3*c*). This organization is still present after surfaces are isolated in sucrose gradients (*a*). After removal of the membrane skeleton with 10 mM NaOH, however, the ridge-and-groove organization is lost (*d*) and the freeze-fracture images (*c*) show no organized pattern on the E (outer leaf, intramembrane) face. The large particles identify the P (inner leaf, intramembrane) face of the plasma membrane and distinguish it from the now unstructured E face. The polypeptide composition of stripped membranes is shown in the SDS gel of *e*, lane *2* (22 μg protein). Two prominent bands of 68 and 39 kD remain membrane associated, whereas most of the other surface polypeptides such as tubulin and the 86- and 80-kD proteins are solubilized (lane *1*, 30 μg protein). Lane *2* represents twice the amount of membrane protein from which the material in lane *1* was extracted. (*a* and *b*) × 107,000; (*c*) × 150,000; (*d*) × 206,000.

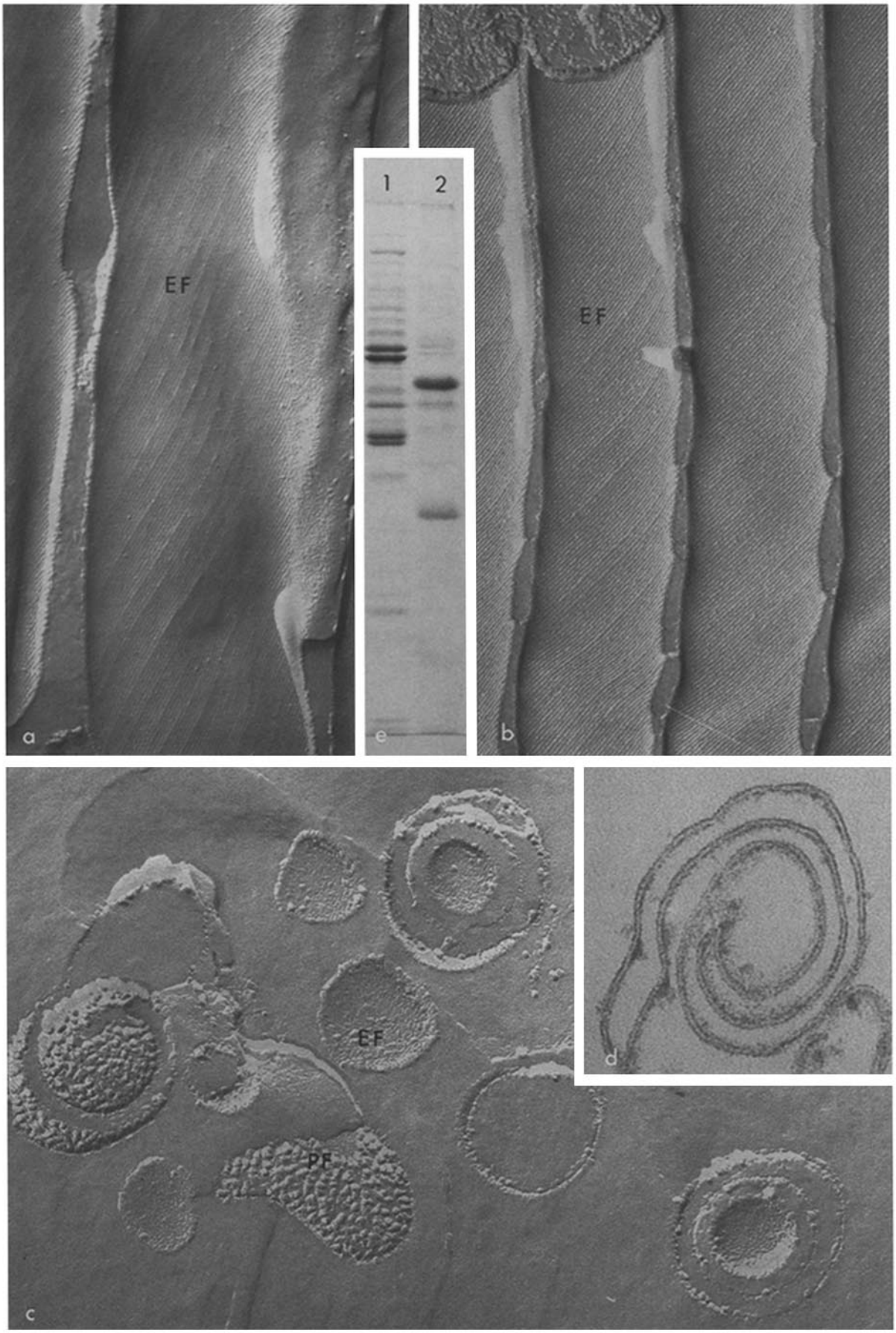
EF
1
2
a
e
EF
b
EF
PF
c
d

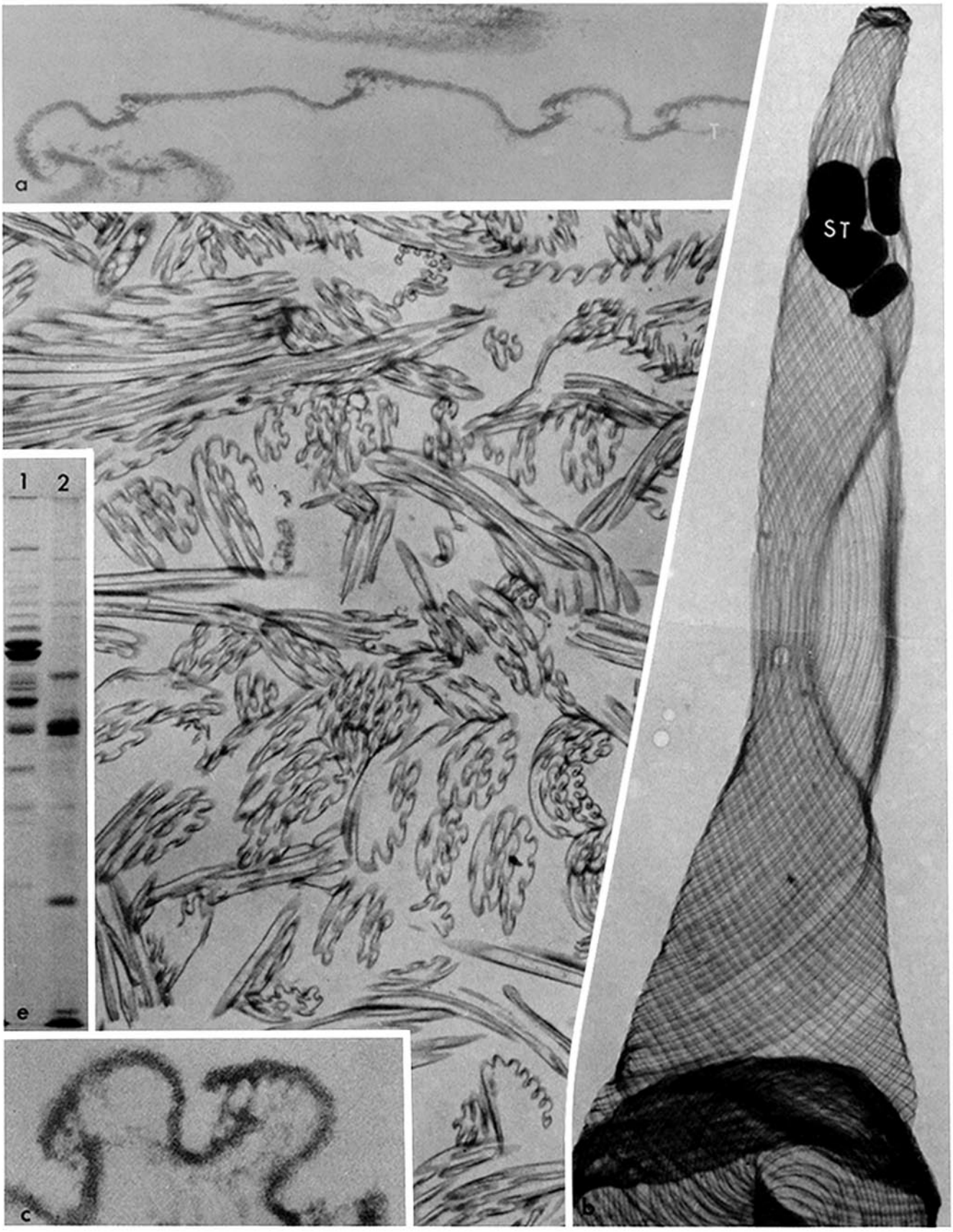
a
T
ST
1
2
e
c
b

TABLE I. *Composition of Cell Surface Fractions*

Surface fraction	Dry wt	Protein (P)	Carbohydrate (C)	Lipid (L)	Recovery (P+C+L)	P/L
	μg	μg	μg	μg		
Untreated	384 (100%)	320 (83%)	33 (8.5%)	63 (16.5%)	108%	5.1
NaOH insoluble	143 (37%)	41 (11%)	29 (7.6%)	29 (7.6%)	69%	1.4
NaOH soluble	260 (67%)	274 (71%)	3 (0.7%)	10 (2.7%)	110%	27.4
Recovery (sol. + insol.)	105%	98%	97%	62%	—	—
LIS/NP-40 insoluble	—*	223 (58%)	18 (4.8%)	—*	—	—

Carbohydrate values are the average of two experiments; all other values are the average of three or more determinations. Carbohydrate and lipid were measured in separate experiments and standardized to the average dry weight of untreated surfaces (384 μg). Percentages are given relative to the dry weight of the untreated fraction.

* See text.

(vs. 4.8% in the LIS/NP-40 insoluble fraction). Dry weight and protein and lipid composition of the detergent-soluble fraction could not be determined due to the relatively small amount of cell surface material and the high concentrations of chaotrope and detergent.

To determine if residual membrane lipids might remain associated with the LIS/NP-40-resistant membrane skeleton, surface isolates were extracted with LIS/NP-40 and subsequently extracted with chloroform/methanol. The lipid fraction was chromatographed on silica gel G plates as previously described (7). None of the phospholipids or sterol-like lipids present in extracts of whole surface isolates or from the LIS/NP-40 soluble fraction could be identified in chromatograms of the membrane skeleton (LIS/NP-40-resistant fraction). The latter did display a spot near the solvent front that co-migrated with authentic NP-40. A more sensitive lipid assay using UDP-[^{3}H]glucose incorporation specifically into lipid glucosides (7) indicated that 98% (two experiments) of the chloroform/methanol-soluble label was present in the LIS/NP-40 extract. We tentatively conclude from all of these results that little or no membrane lipid remains associated with the membrane skeleton. Of the neutral sugar identified in surface isolates about half remains associated with the membrane skeleton (Table I), but these sugars are not extracted with chloroform/methanol.

The Membrane Skeleton in Replicating Surfaces

Replicating surfaces of euglenoids (22, 54) are readily distinguished from nonreplicating surfaces (Fig. 6*a*) in appropriate sections. Daughter strips alternate regularly with parental strips and are initially much smaller than the parental ridges (Fig. 6*b*). Daughter strips contain the complete interstrip complex of microtubules and bridges, so presumably there is no lateral weakness in the surface. Skeletons derived from replicating surfaces clearly show that the attachments between new strips and old are bonded by microtubule independent bridges, which prevent lateral disassociation even after the membrane and microtubules are removed (Fig. 6*c*). Of interest is the fact that the membrane skeleton in newly forming strips is about as thick as in the mature strip. This suggests that the membrane skeletal strips expand at one or both lateral edges, thereby requiring one or both sets of bridges to slide along their opposing strip face.

DISCUSSION

The comparison in Table II of the membrane skeleton of *Euglena* identified in this report and the positionally similar, well-characterized human erythrocyte membrane skeleton (reviewed in references 3, 19, and 33) summarizes the following important points: (*a*) In both cases the cytoskeleton is membrane associated (44), not transcellular. (*b*) The isolated membrane skeleton retains the approximate shape of each living cell (59). (*c*) The membrane skeleton of the erythrocyte can modulate the distribution of surface antigens and of intramembrane particles (11, 43). In *Euglena* the intramembrane domain loses its paracrystallinity (Fig. 4*c*) when the cytoskeleton is removed. Reconstitution experiments indicate that this is at least partially reversible (Dubreuil, R. R., and G. B. Bouck, manuscript in preparation). Moreover, the highly ordered intramembrane particles (29, 38) appear in regions of decreased or restricted surface antigen mobility (22), the surface ridges. The sum of these observations thus suggests an unproven but probable cytoskeleton/surface antigen interrelationship in *Euglena*. (*d*) The absence of the membrane skeleton results in membrane vesiculation in erythrocytes (52) and fragmentation into membrane sheets or unsealed vesicles in the case of *Euglena*, which indicates a membrane stabilizing role for the skeleton in both cells. (*e*) The interaction between the membrane and cytoskeleton is NaOH sensitive in both cases; however, unlike in the eryth-

FIGURE 5 (*a–d*) Membrane skeletons obtained from whole cells or isolated surfaces treated with LIS/NP-40. Whole membrane skeletons retain more or less the overall form of the cell at the time it was frozen. Tears in the cell result probably from ice crystal formation during freezing, and these permit the mostly solubilized cell contents to escape from the cell shell. A few starch grains (*st*) are trapped in this preparation. Membrane skeletons can be collected in large quantities by first isolating surfaces in sucrose gradients and then extracting with LIS/NP-40 (*d*). Details of these isolates reveal that the strips are joined laterally only by the MIBs and the traversing fibers (*T*). Breakage of the latter may permit some flattening of the ridge (*a*). The isolated membrane skeleton has no obvious substructure but does appear to be unevenly distributed to form a splotchy layer or reticulum (a and c). The predominant polypeptides remaining in the skeleton are the 86- and 80-kD bands along with a number of relatively minor components (*e*, lane *1*, 30 μg protein). Solubilized polypeptides include tubulin and the major membrane proteins of 68 and 39 kD (lane *2*, 17 μg protein). The gel samples shown were extracted for only 1 h; complete extraction (≥16 h) removes all of the 68- and 39-kD protein (not shown). Lane *2* represents twice the amount of protein extracted from the material in lane *1*. (*a*) × 64,000; (*b*) × 4,830; (*c*) × 97,000; (*d*) × 36,000.

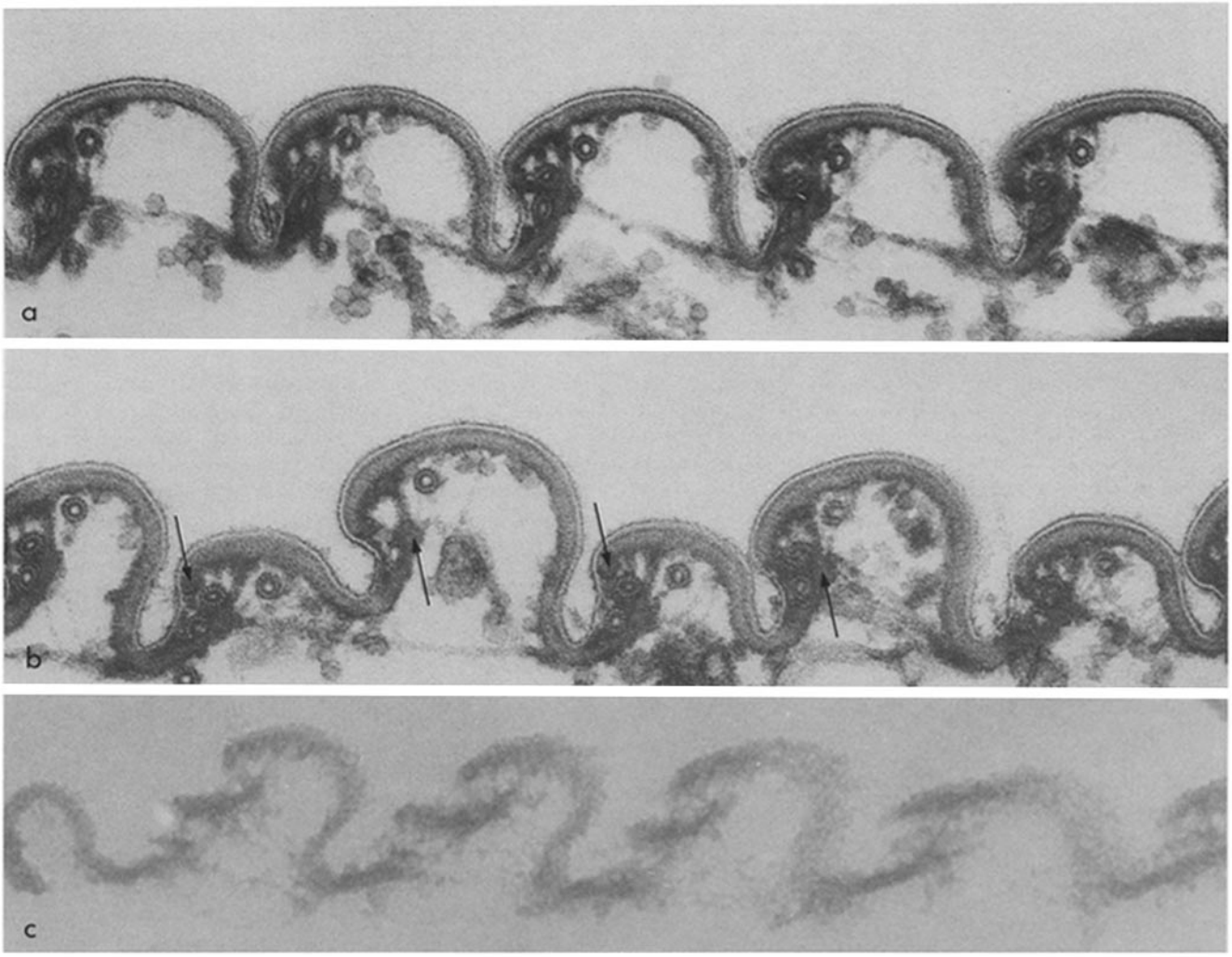

FIGURE 6 Transverse sections through surface isolates that were either nonreplicating (*a*), replicating (*b*), or replicating and extracted with LIS/NP-40 (*c*). In replicating strips (*b*), new strip insertion occurs between parental ridges by interpolation of a new strip of membrane skeleton (between arrows) with the formation of a new set of microtubule-independent and -associated bridges to effect lateral bridging. The thickness of the new membrane skeleton matches that of the parent, which suggests that strips expand laterally at the strip margin(s). LIS/NP-40-derived skeletons of replicating strips are firmly bonded via microtubule-independent bridges to the parental skeleton (*c*). (*a*) × 130,000; (*b*) × 127,000; (*c*) × 118,000.

TABLE II. *Comparison of Selected Properties of the Human Erythrocyte and Euglena Membrane Skeletons*

	Erythrocytes	*Euglena*
Position of cytoskeleton	Submembrane (43)*	Submembrane
Structural role of skeleton	Maintenance of bioconcave disk shape (6, 19, 42, 51)	Maintenance of ridge-and-groove and whole cell shape
Major membrane skeleton proteins	240 and 220 kD (spectrin) up to 75% of protein (19)	86 and 80 kD up to 60% of protein
Surface antigen mobility and intramembrane particle distribution	Restricted via spectrin, ankyrin, etc. (11, 44)	Restricted (22), particles reorient after membrane skeleton is removed
Effect of NaOH extraction	Spectrin solubilized (56)	86 and 80 kD solubilized
Effect of low ionic strength	Spectrin solubilized (35)	No effect
Effect of 25 mM LIS	Spectrin solubilized (56)	No effect

* Numbers in parentheses are reference numbers.

rocyte low ionic strength solutions have no detectable effect on the polypeptide interactions in *Euglena* surface isolates. (*f*) Although LIS releases spectrin from erythrocyte ghosts (56), the cytoskeletal proteins of *Euglena* are not solubilized by this treatment. An LIS effect on the interaction between the *Euglena* cytoskeleton and its membrane binding sites is apparent, however, as an increase in the solubility of the plasma membrane during LIS/NP-40 extraction. NP-40 without LIS does not solubilize the major integral membrane proteins of *Euglena*.

These apparent similarities to the erythrocyte are not evident at the biochemical level. Neither the integral membrane

proteins nor the major membrane skeletal proteins of *Euglena* show obvious homologies to the corresponding proteins in other systems, although the latter conclusion must be regarded as tentative until further evidence from comparative peptide mapping and/or immunological cross-reactivity becomes available. The major membrane glycoproteins of erythrocytes (band 3 and glycophorins) are substantially larger than the integral membrane proteins (68 and 39 kD) of *Euglena*. The major *Euglena* skeletal proteins are clearly not spectrin as it exists in erythrocytes, but there is a consistent stoichiometry of the major polypeptides within both cell types. In *Euglena* the 86- and 80-kD proteins become increasingly enriched as membrane skeletons are purified stepwise, until ultimately they compose almost 60% of the LIS/NP-40-resistant membrane skeleton. Through progressive stages of enrichment the amount of 86- vs. 80-kD polypeptides remains nearly constant. That this equivalence is maintained in reconstituted skeletons (Dubreuil, R. R., and G. B. Bouck, manuscript in preparation) suggests that it is not an artifact of the extraction conditions. Spectrinlike polypeptides have been identified in the skeletons of many cell types (5, 18, 20, 30, 46), but spectrins are not the only means of constructing membrane skeletons, as has been demonstrated in lower (32, 58) and higher (17, 34, 45, reviewed in reference 16) eucaryotic cells. Among euglenoids themselves the major *Euglena* polypeptides are markedly different from those reported for the related organism *Distigma proteus* (41), perhaps because the latter displays a prominent surface coat (28) external to the plasma membrane, which is absent in *Euglena*. We have not yet resolved a supramolecular organization for the membrane skeleton; it appears to be formless and isotropic in thin sections and after negative staining. The fibrous material previously attributed to the submembrane layer (29) seems better explained as the traversing fibers viewed from the cytoplasmic side, since the periodicity of the traversing fibers in our preparations is similar to that of the fibrous material found in replicas of freeze-fractured membranes (29).

Although many euglenoids can undergo rapid and extreme shape changes the cellular and molecular explanation for this form of motility has remained elusive. From the present findings it appears that euglenoid shape changes are mirrored in the membrane skeleton, and that preparations from which all other components have been extracted retain that shape immobilized (for example) by rapid freezing. We have provided direct evidence that the membrane skeleton consists of interlocking strips arranged in a manner generally consistent with a suggestion of surface articulation originally made by Leedale (27) for whole cells of *E. spirogyra*. Recent evidence strongly suggests that surface strips slide relative to one another during euglenoid movements (57). It would therefore be reasonable to expect that the motive force for this sliding is localized at the interstrip junction, and it is just this region that appears in the present study to consist of remarkably complex bridgework. Since these bridges superficially resemble flagellar arms consisting of dynein ATPases, and a Mg^{2+} dependent ATPase has been identified in cell surface isolates of the euglenoid *Astasia longa* (40) it seemed that the microtubule-independent bridges in the present study might be analogous to dynein bridges. Unlike dynein, however, the microtubule-independent bridges are not disassociated under high salt conditions, and no high molecular weight polypeptide corresponding to dynein could be identified in significant quantities on acrylamide gels of isolated surfaces. The microtubule-independent bridges of the isolated skeleton are difficult to disrupt, and except for mechanical shear we have found no extraction protocol that will separate skeletons into individual strips.

Yet in the living cell it seems likely that individual strips must be free to undergo controlled sliding along the strip margins. Such sliding has been recorded by video microscopy in the euglenoid *E. fusca* (57), in which the prominent surface ornamentation is especially useful for marking the position of one strip relative to another both spatially and temporally. In these cells strips are immobilized at their anterior and posterior termini but may slide bidirectionally several micrometers past one another near the cell center during euglenoid movements. If we assume that *E. gracilis* of the present report moves by a similar mechanism, then the microtubule-independent bridges of the skeleton must be able to accommodate locally or implement long stretches of bidirectional sliding. An actin-based mechanism has been proposed to explain movement (14), but such a model would require that the motive force be removed from the immediate cell surface, since no 43-kD actinlike protein has been identified in acrylamide gels of surfaces from *A. longa* (40) or *E. gracilis* (present study). Because a strip-sliding model based on actin would still require adjustment of individual bridges during movement, we favor the hypothesis that the strip bridgework and/or adjacent microtubules are the site of force generation whereas the position of the strips relative to one another determines whole cell form. Traversing fibers may then provide an elastic restraint to the extent of strip sliding.

Overall, these cells seem to have a surface construct well able to accommodate current interpretations of euglenoid motility (57) and replication (22). As a working hypothesis we propose that the membrane skeletal strips are the basic unit of surface organization, the basic unit of surface replication, and the functional unit in surface deformation in euglenoids. If these properties are substantiated, the euglenoids should become particularly useful models for analyzing membrane/cytoskeletal interactions and surface movements.

This work was supported by a University of Illinois Graduate Fellowship to R. R. Dubreuil and National Science Foundation grant PCM8203442 to G. B. Bouck.

Received for publication 14 November 1984, and in revised form 25 June 1985.

REFERENCES

1. Bell, C. W., C. Fraser, W. S. Sale, W.-J. Y. Tang, and I. R. Gibbons. 1982. Preparation and purification of dynein. *Methods Cell Biol.* 24:373–397.
2. Bouck, G. B. 1982. Flagella and the cell surface. *In* The Biology of *Euglena*, Vol. 3. D. E. Buetow, editor. Academic Press, Inc., New York. 29–51.
3. Branton, D. 1981. Membrane cytoskeletal interactions in the human erythrocyte. *Cold Spring Harbor Symp. Quant. Biol.* 46:1–5.
4. Buetow, D. E. 1968. Morphology and ultrastructure of *Euglena*. *In* The Biology of *Euglena*, Vol. 1. D. E. Buetow, editor. Academic Press, Inc., New York. 110–184.
5. Burridge, K., T. Kelly, and P. Mangeat. 1982. Nonerythrocyte spectrins: actin-membrane attachment proteins occuring in many cell types. *J. Cell Biol.* 95:478–486.
6. Carter, D. P., and G. Fairbanks. 1984. Inhibition of erythrocyte membrane shape change by band 3 cytoplasmic fragment. *J. Cell. Biochem.* 24:385–393.
7. Chen, S. J., and G. B. Bouck. 1984. Endogenous glycosyltransferases glucosylate lipids in flagella of *Euglena*. *J. Cell Biol.* 98:1825–1835.
8. Cogburn, J. N., and J. A. Schiff. 1984. Purification and properties of the mucus of *Euglena gracilis* (Euglenophyceae). *J. Phycol.* 20:533–544.
9. Dressler, V., C. W. M. Haest, G. Plasa, B. Dueticke, and J. D. Erusalimsky. 1984. Stabilizing factors of phospholipid asymmetry in the erythrocyte membrane. *Biochim. Biophys. Acta.* 775:189–196.
10. Dubois, M., K. A. Gilles, J. K. Hamilton, P. A. Rebers, and F. Smith. 1956. Colorimetric method for determination of sugars and related substances. *Anal. Chem.* 28:350–356.
11. Elgsaeter, A., and D. Branton. 1974. Intramembrane particle aggregation in erythrocyte ghosts. I. The effects of protein removal. *J. Cell Biol.* 63:1018–1030.

12. Ferrel, J. E., and W. H. Huestis. 1984. Phosphoinositide metabolism and the morphology of human erythrocytes. *J. Cell Biol.* 98:1992–1998.
13. Gallo, J.-M., E. Karsenti, M. Bornens, A. Delacourte, and J. Schrevel. 1982. Euglenoid movement in *Distigma proteus*. II. Presence and localization of an actin-like protein. *Biol. Cell.* 44:149–156.
14. Gallo, J.-M., and J. Schrevel. 1982. Euglenoid movement in *Distigma proteus*. I. Cortical rotational motion. *Biol. Cell.* 44:139–148.
15. Geetha-Habib, M., and G. B. Bouck. 1982. Synthesis and mobilization of flagellar glycoproteins during regeneration in *Euglena*. *J. Cell Biol.* 93:432–441.
16. Geiger, B. 1983. Membrane-cytoskeleton interaction. *Biochim. Biophys. Acta.* 737:305–341.
17. Glenney, J. R., Jr., and P. Glenney. 1984. The microvillus 110K cytoskeletal protein is an integral membrane protein. *Cell.* 37:743–751.
18. Glenney, J. R., Jr., P. Glenney, M. Osborn, and K. Weber. 1982. An F-actin and calmodulin-binding protein from isolated intestinal brush borders has a morphology related to spectrin. *Cell.* 28:843–854.
19. Goodman, S., and K. Shiffer. 1983. The spectrin membrane skeleton of normal and abnormal human erythrocytes: a review. *Am. J. Physiol.* 244 (*Cell Physiol.* 13): c121–c141.
20. Goodman, S. R., I. S. Zagon, and R. R. Kulikowski. 1981. Identification of a spectrin-like protein in nonerythroid cells. *Proc. Natl. Acad. Sci. USA.* 78:7570–7574.
21. Gunning, B. E. S., and A. R. Hardham. 1982. Microtubules. *Annu. Rev. Plant Physiol.* 33:651–698.
22. Hoffman, C., and G. B. Bouck. 1976. Immunological and structural evidence for patterned intussusceptive surface growth in a unicellular organism. *J. Cell Biol.* 69:693–715.
23. Jinbu, Y., S. Sato, T. Nakao, M. Nakao, S. Tsukita, S. Tsukita, and H. Ishikawa. 1984. The role of ankyrin in shape and deformability change of human erythrocyte ghosts. *Biochim. Biophys. Acta.* 773:237–245.
24. Lange, Y., A. Gough, and T. L. Steck. 1982. Role of the bilayer in the shape of the isolated erythrocyte membrane. *J. Membr. Biol.* 69:113–123.
25. Lange, Y., R. A. Hadesmon, and T. L. Steck. 1982. Role of the reticulum in the stability and shape of the isolated human erythrocyte membrane. *J. Cell Biol.* 92:714–721.
26. Lebkowski, J. S., and U. K. Laemmli. 1982. Non-histone proteins and long-range organization of HeLa interphase DNA. *J. Mol. Biol.* 156:325–344.
27. Leedale, G. F. 1964. Pellicle structure in *Euglena*. *Br. Phycol. Bull.* 2:291–306.
28. Leedale, G. F. 1967. Euglenoid Flagellates. Prentice-Hall Inc., Englewood Cliffs, NJ. 242 pp.
29. Lefort-Tran, M., M. H. Bré, J. L. Ranck, and M. Pouphile. 1980. *Euglena* plasma membrane during normal and vitamin B_{12} starvation growth. *J. Cell Sci.* 41:245–261.
30. Levine, J., and M. Willard. 1981. Fodrin: axonally transported polypeptides associated with the internal periphery of many cells. *J. Cell Biol.* 90:631–643.
31. Lowry, O. H., N. J. Rosebrough, A. L. Farr, and R. J. Randall. 1951. Protein Measurements with the Folin phenol reagent. *J. Biol. Chem.* 193:265–275.
32. Luna, E. J., C. M. Goodloe-Holland, and H. M. Ingalls. 1984. A membrane cytoskeleton from *Dictyostelium discoideum*. II. Integral proteins mediate the binding of plasma membranes to F-actin affinity beads. *J. Cell Biol.* 99:58–70.
33. Lux, S. E. 1979. Spectrin-actin membrane skeleton of normal and abnormal red blood cells. *Semin. Hematol.* 16:21–50.
34. Mangeat, P., and K. Burridge. 1984. Actin-membrane interaction in fibroblasts: what proteins are involved in this association? *J. Cell Biol.* 99(1, Pt. 2):95s–103s.
35. Marchesi, V. T. 1974. Isolation of spectrin from erythrocyte membranes. *Methods Enzymol.* 32:275–277.
36. Marchesi, V. T., and E. P. Andrews. 1971. Glycoproteins: isolation from cell membranes with lithium diiodosalicylate. *Science (Wash. DC).* 174:1247–1248.
37. Mignot, J.-P. 1966. Structure et ultrastructure de quelques Euglénomonadines. *Protistologica.* 2(3):51–117.
38. Miller, K. R., and G. J. Miller. 1978. Organization of the cell membrane in *Euglena*. *Protoplasma.* 95:11–24.
39. Mizuhira, V., and Y. Futaesaku. 1972. New fixation for biological membranes using tannic acids. *Acta Histochem. Cytochem.* 5:233–235.
40. Murray, J. M. 1981. Control of cell shape by calcium in the Euglenophyceae. *J. Cell Sci.* 49:99–117.
41. Murray, J. M. 1984. Disassembly and reconstitution of a membrane-microtubule complex. *J. Cell Biol.* 98:1481–1487.
42. Nelson, G. A., M. L. Andrews, and M. J. Karnovsky. 1983. Control of erythrocyte shape by calmodulin. *J. Cell Biol.* 96:730–735.
43. Nicolson, G. L., V. T. Marchesi, and S. J. Singer. 1971. Localization of spectrin on the inner surface of human red blood cell membranes by ferritin conjugated antibodies. *J. Cell Biol.* 51:265–272.
44. Nicolson, G. L., and R. G. Painter. 1973. Anionic sites of human erythrocyte membranes. II. Antispectrin-induced transmembrane aggregation of the binding sites for positively charged colloidal particles. *J. Cell Biol.* 59:395–406.
45. Pardo, J. V., J. D'Angelo Siliciano, and S. W. Craig. 1983. A vinculin-containing cortical lattice in skeletal muscle: transverse lattice elements ("costameres") mark sites of attachment between myofibrils and sarcolemma. *Proc. Natl. Acad. Sci. USA.* 80:1008–1012.
46. Repasky, E. A., B. L. Granger, and E. Lazarides. 1982. Widespread occurrence of avian spectrin in nonerythroid cells. *Cell.* 29:821–833.
47. Rogalski, A. A., and G. B. Bouck. 1980. Characterization and localization of a flagellar-specific membrane glycoprotein in *Euglena*. *J. Cell Biol.* 86:424–435.
48. Rosenbaum, J. L., and F. M. Child. 1967. Flagella regeneration in protozoan flagellates. *J. Cell Biol.* 34:345–364.
49. Seigneuret, M., and P. F. Devaux. 1984. ATP-dependent asymmetric distribution of spin-labeled phospholipids in the erythrocyte membrane: relation to shape changes. *Proc. Natl. Acad. Sci. USA.* 81:3751–3755.
50. Sheetz, M. P., and S. J. Singer. 1974. Biological membranes as bilayer couples. A molecular mechanism of drug-erythrocyte interactions. *Proc. Natl. Acad. Sci. USA.* 71:4457–4461.
51. Sheetz, M. P., and S. J. Singer. 1977. On the mechanism of ATP-induced shape-changes in human erythrocyte membranes. I. The role of the spectrin complex. *J. Cell Biol.* 73:638–646.
52. Shohet, S. B. 1979. Reconstitution of spectrin-deficient spherocytic mouse erythrocyte membranes. *J. Clin. Invest.* 64:483–493.
53. Silverman, H., and R. S. Hikida. 1976. Pellicle complex of *Euglena gracilis*: characterization by disruptive treatments. *Protoplasma.* 87:237–252.
54. Sommer, J. R., and J. J. Blum. 1964. Pellicular changes during cell division in *Astasia longa*. *Exp. Cell Res.* 35:423–425.
55. Spurr, A. R. 1969. A low-viscosity epoxy resin embedding medium for electron microscopy. *J. Ultrastruct. Res.* 26:31–43.
56. Steck, T. L., and J. Yu. 1973. Selective solubilization of proteins from red blood cell membranes by protein perturbants. *J. Supramol. Struct.* 1:220–232.
57. Suzaki, T., and R. E. Williamson. 1985. Euglenoid movement in *Euglena fusca*: evidence for sliding between pellicular strips. *Protoplasma.* 124:137–146.
58. Williams, N. E., P. E. Vaudaux, and L. Skriver. 1979. Cytoskeletal proteins of the cell surface in *Tetrahymena*. I. Identification and localization of major proteins. *Exp. Cell Res.* 123:311–320.
59. Yu, J., D. A. Fischman, and T. L. Steck. 1973. Selective solubilization of proteins and phospholipids from red blood cell membranes by nonionic detergents. *J. Supramol. Struct.* 1:233–248.